2016

Comparative Analysis of Two Types of Positive Displacement Compressors for Air Conditioning Applications

Marco Carrilho Diniz
POLO - UFSC, Brazil, marcodiniz@polo.ufsc.br

Cesar Jose Deschamps
POLO - UFSC, Brazil, deschamps@polo.ufsc.br

Comparative Analysis of Two Types of Positive Displacement Compressors for Air Conditioning Applications

Marco C. DINIZ[1], Cesar J. DESCHAMPS[1]*

[1]POLO Research Laboratories for Emerging Technologies in Cooling and Thermophysics
Federal University of Santa Catarina
Florianopolis, SC, Brazil
deschamps@polo.ufsc.br

* Corresponding Author

ABSTRACT

Different types of positive displacement compressors are employed in low-capacity air conditioning applications. Understanding the advantages and drawbacks of each of these technologies is important in order to identify the ranges of cooling capacities at which a specific compression technology is more efficient. This paper presents a comparative analysis between two positive displacement compressors (rolling piston and scroll) designed for air conditioning applications. The compressors operate with R-22 and present a nominal cooling capacity of 18000 BTU/h at the AHRI-A checkpoint condition. First, the compressors were tested in a hot-cycle test bench to measure the mass flow rate and power consumption for MBP and HBP operating conditions. The results showed that the most efficient compressor depends on the operating condition. After this, simulation models for each compressor were validated against the experimental data, showing good agreement. Therefore, through the simulation models, it was possible to evaluate the effect of different aspects, such as leakage, heat transfer and discharge process, on the efficiency of each compressor.

1. INTRODUCTION

A significant percentage of the energy used in buildings is related to air conditioning systems, especially in tropical climates (Chua *et al.*, 2013). Most of these systems employ the vapor compression refrigeration cycle, in which the compressor is the main component when it comes to electrical power consumption. Therefore, to improve the performance of the whole system it is necessary to employ efficient compressors.

The first generations of air conditioning systems used in small and medium size applications employed reciprocating compressors. Gradually, with the advent of rotary compressors, reciprocating compressors were increasingly replaced by rolling piston and scroll compressors, which presented higher efficiency and reliability. Nowadays, rolling piston and scroll compressors are widely spread and dominate the market for small and medium size air conditioning systems. Nevertheless, it should also be mentioned that some researchers (Ooi, 2014; Orosz *et al.*, 2014) are continuously working to develop new types of compressors that overcome the main drawbacks associated with rotary compressors.

The global efficiency of hermetic compressors is related to its electrical, mechanical and thermodynamic performances. The electrical motor design is one of the most important aspects when defining the compressor operating envelope and the research on this subject is usually focused on motor reliability. The studies related to the mechanical behavior of rolling piston and scroll compressors dominated the research efforts in the beginning of their technical development, when the objective was to develop durable and reliable compressors. As the electrical and mechanical improvements of the compressors are usually limited by cost, the detailed analysis of the thermodynamic phenomena is fundamental in order to identify opportunities to increase compressor global efficiency.

Several works have been developed regarding the thermodynamic performance of both rolling piston (Ooi, 2012) and scroll compressors (Maertens and Richardson, 1992), usually with focus on the impact of using different refrigerants. On the other hand, few works (Gomes and Deschamps, 2007) have been conducted with the objective of comparing the thermodynamic efficiency of these compressors. However, the comparative thermodynamic analysis of these compressors is important to identify the advantages and drawbacks of each technology.

This work presents a comparative analysis of the thermodynamic efficiency of a rolling piston and a scroll compressor operating under MBP and HBP applications. Two compressors with similar volumetric displacements were tested in a hot-cycle test bench in nine operating conditions. Simulation models were adjusted for each compressor, validated against experimental data, and used to evaluate and compare their energy and mass losses under different operating conditions.

2. EXPERIMENTAL PROCEDURE

The rolling piston and scroll compressors evaluated in this work were tested with their original shells, i.e., no internal measurements were possible. Externally, the compressors were instrumented with a thermocouple to measure the shell temperature, which was used to establish a criterion for thermal stabilization during the measurements. Both compressors used refrigerant R22 and operated at 60 Hz. The displacement volume of the rolling piston compressor was 23.9 cm^3, while for the scroll the displacement volume was 25.2 cm^3.

The compressors were tested in a hot-cycle test bench, in which all the thermodynamic processes occur with the gas in the superheated vapor state. In this facility, a set of micrometric valves is adopted to submit the compressor to the required pressure ratio, while the temperature at the compressor suction line is controlled through heat exchangers. A coriolis mass flow meter and a power transducer available in the test bench allowed the measurements of mass flow rate and power consumption, respectively. Details about the operation of such a test bench are available in Dutra and Deschamps (2013).

The tests were performed under nine operating conditions defined by the combination of three evaporating temperatures (-1.1ºC, 7.2ºC and 12.8ºC) and three condensing temperatures (37.8ºC, 48.9ºC and 60.0ºC). For all conditions, the temperature in the compressor inlet was set to be 8.3ºC higher than the evaporating temperature. Each test was stopped when the compressor was considered thermally stabilized. This condition was achieved when during 30 minutes the temperature of the compressor shell showed a maximum variation of ± 0.5˚C. Then, the next 30 minutes of the test were used to calculate the average mass flow rate and power consumption. Three repetitions were conducted for each operating condition, showing good repeatability. With the average mass flow rate, power consumption and temperature at the compressor inlet, the main performance parameters for the nine operating conditions can be calculated.

Tables 1 and 2 present two dimensionless important performance indicators of rolling piston and scroll compressors. Table 1 presents the volumetric efficiency $\eta_v = \dot{m}/\dot{m}_{th}$, where $\dot{m}$ is the measured mass flow rate and $\dot{m}_{th}$ is the theoretical mass flow rate. Table 2 shows the global efficiency $\eta_g = \dot{W}_{th}/\dot{W}_{ele}$, where $\dot{W}_{th}$ is the theoretical power of isentropic compression, estimated taking into account the measured mass flow rate, and $\dot{W}_{ele}$ is the measured electrical power consumption.

Table 1 – Experimental results of volumetric efficiency for rolling piston and scroll compressors

Volumetric efficiency [%]		T_e [ºC]								
		-1.1			7.2			12.8		
		Rolling piston	Scroll	Difference [%]	Rolling piston	Scroll	Difference [%]	Rolling piston	Scroll	Difference [%]
T_c [ºC]	37.8	90.6	90.8	+0.2	91.3	92.8	+1.6	93.0	94.0	+1.1
	48.9	87.4	88.4	+1.1	88.6	90.7	+2.4	89.6	92.0	+2.7
	60.0	83.1	81.2	-2.3	84.9	87.4	+2.9	85.8	89.3	+4.1

Table 2 – Experimental results of global efficiency for rolling piston and scroll compressors

Global efficiency [%]		T_e [ºC]								
		-1.1			7.2			12.8		
		Rolling piston	Scroll	Difference [%]	Rolling piston	Scroll	Difference [%]	Rolling piston	Scroll	Difference [%]
T_c [ºC]	37.8	65.2	64.5	-1.1	63.2	64.7	+2.4	61.1	61.5	+0.7
	48.9	64.5	61.8	-4.2	64.8	66.2	+2.2	65.0	67.1	+3.2
	60.0	59.7	52.4	-12.2	61.4	61.4	+0.0	62.9	64.9	+3.2

As expected, it can be observed that the operating condition is important to define the most efficient compressor. The scroll compressor is more efficient than the rolling piston compressor both in terms of volumetric and global efficiency in the two higher evaporating temperatures analyzed, especially closer to its internal pressure ratio. However, for the lower evaporating temperature, the rolling piston becomes more competitive even overcoming the performance of the scroll compressor. This aspect is more pronounced at the condition with the higher pressure ratio, where the global efficiency of the rolling piston is more than 10% higher than that of the scroll compressor. These experimental results are useful to establish which compressor presents the best performance in each condition. However, as internal measurements were not performed, it was not possible to clearly identify the reasons for the differences of thermodynamic performance between the two compressors. In order to allow such an analysis, two simulation models were employed and will be described in the next section.

3. MATHEMATICAL MODELS

The models used to simulate the compression cycles of both rolling piston and scroll compressors are based on a transient lumped formulation, which allows the calculation of the thermodynamic properties of the gas throughout the suction, compression and discharge processes. This procedure is based on a method widely employed in the literature, where four groups of equations are used to characterize the whole compression cycle. The solution procedure for each model will be briefly described herein. Further information regarding the models can be found in Brancher (2013) for the rolling piston compressor and Pereira and Deschamps (2010) for the scroll compressor.

The first group of equations is used to calculate the instantaneous volume of the suction, compression and discharge chambers, which depend solely on the geometrical parameters of each compression mechanism. For the rolling piston compressor these parameters include the cylinder, piston and blade dimensions, whereas for the scroll compressor the number of turns of the scroll wrap and its dimensions are required. To estimate these parameters both compressors were opened and the important data were measured with appropriate instruments.

The second group of equations is the conservation equations for the volumes formed by the compressor chambers. As the instantaneous volume of the chambers is known, to estimate the instantaneous density a mass balance is necessary:

$$\frac{dm_g}{dt} = \sum \dot{m}_{in} - \sum \dot{m}_{out} \tag{1}$$

where the summations of instantaneous mass flow rates include those in the suction and discharge orifices and also the ones due to leakage through clearances. An energy balance, Equation (2), is used to calculate the instantaneous temperature during the compression cycle. With the density and the temperature being evaluated via Equations (1) and (2), it is possible to obtain the refrigerant instantaneous pressure by employing an equation of state.

$$\frac{dT_g}{dt} = \frac{1}{m_g c_v}\left\{-T_g\left(\frac{\partial p_g}{\partial T_g}\right)_{\forall} - \frac{1}{\rho_g}\frac{dm_g}{dt} - \sum \dot{m}_{in}\left(h_g - h_{in}\right) + H_g\left(T_w - T_g\right)\right\} \tag{2}$$

In Equation (2), H_g and T_w are, respectively, the convective heat transfer coefficient and the temperature at the cylinder wall (for the rolling piston) or at scroll wrap (for the scroll), while h_{in} is the enthalpy of the gas entering the chamber. During the formation of the suction chamber of both compressors, this temperature is very important to characterize the so-called suction gas superheating, which is known to affect compressor efficiency.

For the rolling piston compressor, H_g was calculated using the correlation employed by Liu and Soedel (1992). The cylinder temperature was considered equal to the shell temperature, for which experimental measurements in the nine different conditions were available. This decision was considered acceptable, as the cylinder and shell temperature are quite similar for a high pressure shell rolling piston compressor (Padhy, 1994). The suction temperature was estimated by calculating the heat transfer in the suction passage with the $\epsilon - NTU$ method, in which the cylinder was considered as the heat source.

For the scroll compressor model, H_g is estimated using a correlation developed from the numerical simulations presented by Pereira and Deschamps (2012), whereas the suction temperature was calculated following the procedure presented by Diniz and Deschamps (2014). The temperature of the scroll wraps was estimated by considering a linear profile from its most outer point up to the most central point. Based on the results of Jang and Jeong (2004), the lowest temperature of the scroll was considered to be 15ºC higher than the suction temperature and the highest temperature of the scroll was set to be 10ºC lower than the average discharge temperature of the gas.

The third group of equations is required to predict valve dynamics. A single degree-of-freedom mass spring model was employed to calculate the discharge valve dynamics of the rolling piston. Effective force areas were previously obtained through CFD simulations to predict the force acting on the valve during the compression cycle.

Finally, the fourth group of equations predicts the mass flow rate through the suction and discharge orifices and the gas leakage through clearances. For the rolling piston, the mass flow rate through the suction and discharge orifices was estimated with reference to an isentropic flow through a convergent nozzle, which was corrected via the concept of effective flow areas. Different models were employed to calculate leakage through the clearances of the rolling piston compressor, and details can be obtained in Bezerra Jr *et al.* (2013). For the scroll compressor, the mass flow into the suction pocket was estimated using the correlation developed by Pereira (2012), while the mass flow through the discharge orifice was calculated with the concept of effective flow areas. The leakages through the flank and top clearances were predicted by using the correlations presented by Pereira and Deschamps (2015).

Both models were simulated for a certain number of cycles until the compressor operating conditions were cyclically repeated, allowing the predictions of the main performance parameters and the inventories of energy and mass losses.

4. RESULTS

Before using the models to predict the mass and energy losses of the compressors, some numerical predictions were validated through comparisons with the available experimental data. Table 3 presents the differences between predictions and measurements of mass flow rate, showing that the error is smaller than 2% in most of the conditions analyzed. To achieve such an agreement for the mass flow rate it was necessary to adjust the clearances of the scroll for each of the conditions.

Table 3 – Errors associated with predictions of mass flow rate.

Error in mass flow rate [%]		**T_e [ºC]**					
		-1.1		**7.2**		**12.8**	
		Rolling piston	**Scroll**	**Rolling piston**	**Scroll**	**Rolling piston**	**Scroll**
T_c [ºC]	**37.8**	-1.66	-0.11	-0.04	+0.40	-0.47	+0.14
	48.9	-0.85	+0.12	+0.51	+0.64	+1.03	+0.79
	60.0	+0.93	+4.25	+1.80	+0.38	+2.64	+0.48

Table 4 shows the errors associated with the power consumption prediction. This parameter was numerically estimated by using the numerical indicated power and values of electromechanical efficiency adjusted for each condition for both compressors. The agreement between experimental and numerical results can be considered satisfactory.

Table 4 – Errors associated with predictions of power consumption

Error in power consumption [%]		T_e [ºC]					
		-1.1		7.2		12.8	
		Rolling piston	Scroll	Rolling piston	Scroll	Rolling piston	Scroll
T_c [ºC]	37.8	0.64	-2.21	-0.64	-0.23	+1.25	-0.20
	48.9	0.46	-0.65	0.17	+0.18	+0.21	+0.89
	60.0	0.87	-1.04	0.00	+1.02	-0.73	+2.33

To extrapolate the analysis to other operating conditions, it was necessary to obtain curves that estimate the variation of the aforementioned adjusted parameters within the envelope. For each operating condition of the rolling piston, the electromechanical efficiency and the cylinder temperature (necessary to calculate the suction temperature and to estimate heat transfer inside the chamber) were expressed as a function of the evaporating and condensing temperatures. A similar approach was employed for the scroll compressor in order to predict the clearances and the electromechanical efficiency throughout the application envelope. The results shown hereafter were obtained by using such curves.

Figures 1 and 2 present the suction and discharge temperatures of the rolling piston and scroll compressors at different condensing temperatures, for the three evaluated evaporating temperatures. As in the scroll compressor the gas that enters the shell fills the internal environment before flowing to the suction chamber, its suction temperature is higher than that of the rolling piston. However, the discharge temperatures of the rolling piston are higher than those of the scroll compressor for most of operating conditions.

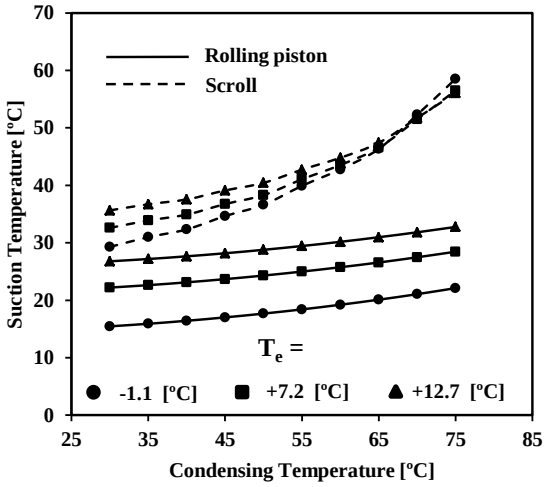

Figure 1: Suction temperature of rolling piston and scroll compressor

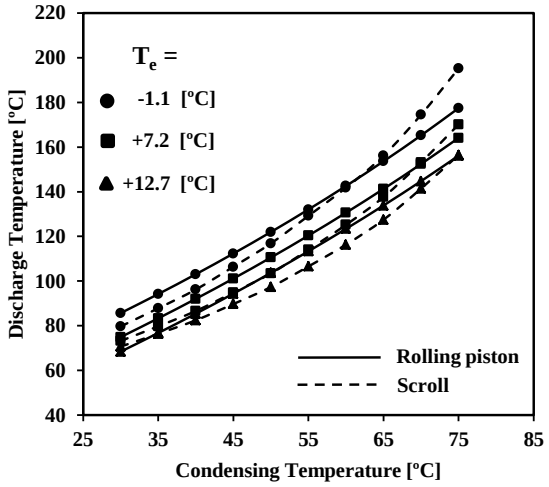

Figure 2: Discharge temperature of rolling piston and scroll compressor

Figures 3 and 4 present the indicated power and the thermodynamic efficiency of the rolling piston and scroll compressors at different condensing temperatures for the three evaluated evaporating temperatures. The indicated powers of both compressors have the same order of magnitude, with a monotonic increase with the pressure ratio π (= p_c/p_e). However, Figure 4 show that the thermodynamic efficiency of the scroll compressor is much more sensitive to changes in the operating condition, with a considerable decrease of efficiency when applied far from its design operating condition, which corresponds the condition in which the system pressure ratio matches the internal

pressure ratio of the compressor. In fact, the efficiency of the scroll compressor is higher than that of the rolling piston in the design condition. On the other hand, the rolling piston compressor presents a more flat behavior for the thermodynamic efficiency throughout the operating conditions analyzed.

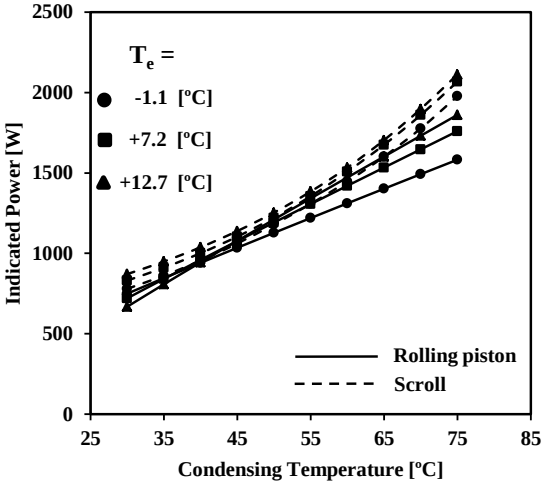

Figure 3: Indicated power of rolling piston and scroll compressor for different evaporating temperatures.

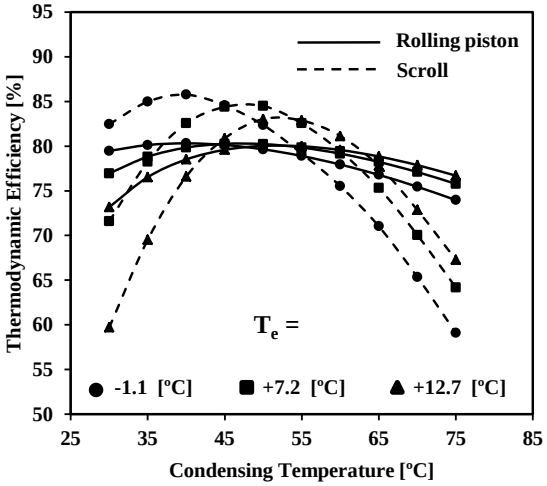

Figure 4: Thermodynamic efficiency of rolling piston and scroll compressor for different evaporating temperatures.

The inventory of energy losses is a convenient way of identifying the reasons for the trends shown in Figure 4. Figures 5 and 6 present the energy losses associated with the compression cycle of the rolling piston for evaporating temperatures of T_e = -1.1ºC and T_e = +12.7ºC at different condensing temperatures. The energy loss due to viscous friction in the suction orifice was not significant and therefore was neglected.

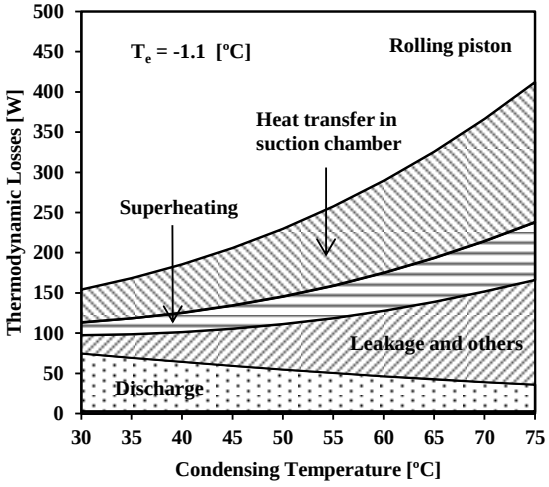

Figure 5: Thermodynamic losses for the rolling piston compressor at T_e = -1.1 ºC

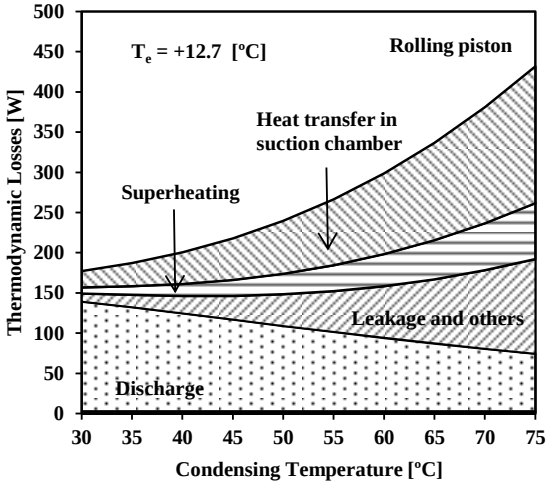

Figure 6: Thermodynamic losses for the rolling piston compressor at T_e = 12.7 ºC

It can be observed that total thermodynamic loss is more dependent on the condensing temperature than on the evaporating temperature. The impact of heat transfer was divided in two contributions: the loss due to the increase in refrigerant temperature from the suction line until the suction port (superheating) and the loss associated with the increase in refrigerant temperature from the suction port until the beginning of the compression process (heat transfer in suction chamber). In the rolling piston, due to the small path of the suction tube, the increased amount of work due to suction superheating is small when compared to the increase caused by heat transfer during the

formation of the suction chamber, which is mainly associated with the adopted high-pressure shell design. As expected, the energy losses due to leakage are more pronounced at higher pressure ratios. The losses in the discharge process are more significant at higher evaporating and low condensing temperatures because under these conditions the mass flow rate is higher, increasing the flow velocity and viscous losses in the discharge valve.

The diagrams depicting the scroll compressor thermodynamic losses are shown in Figures 7 and 8. For this compressor, the thermodynamic losses are considerably influenced by under and over compression. Such losses occur because the initial pressure in the discharge pocket is governed by the suction pressure and the compressor internal pressure ratio, regardless of the condensing pressure. The under compression loss occurs if the discharge pocket initial pressure is lower than that of the condenser, resulting in backflow from the compressor discharge plenum to the discharge pocket. When this high pressure refrigerant re-enters the discharge pocket, the volume of the chamber is still decreasing and therefore this gas is compressed again. This process will continue until the gas in the discharge pocket reaches a slightly higher pressure than that of the discharge plenum, when the gas is finally discharged. This phenomenon was incorporated into the leakage contribution of the thermodynamic losses and is more pronounced at higher condensing temperatures, especially for the lower evaporating temperature (Figure 7). A solution commonly employed to minimize the under compression loss is to use a discharge valve, although it increases the viscous losses of the discharge process.

If the pressure in the discharge pocket is above the condensing pressure, then the compressor is operating with over compression as the compression process required more energy than the one that would be necessary to match the system pressure ratio. This loss, identified as a discharge loss in Figure 8, is considerable for the lower condensing temperatures. By comparing Figures 7 and 8 it is possible to identify that the point of lowest thermodynamic losses occurs at higher condensing temperatures when the evaporating temperature is increased, following the compressor internal pressure ratio. These aspects show that the design of scroll compressors is strongly dependent on the operating conditions determined by the system.

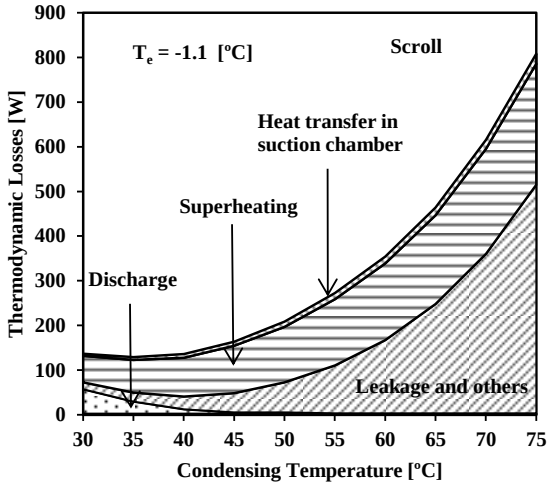

Figure 7: Thermodynamic losses for scroll compressor at T_e = -1.1 ºC

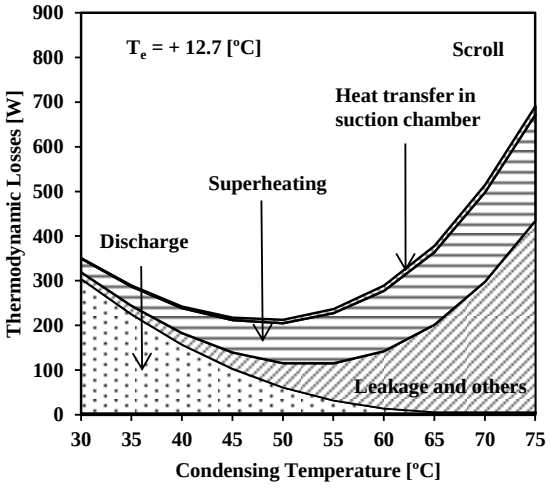

Figure 8: Thermodynamic losses for scroll compressor at T_e = 12.7 ºC

The diagrams of energy losses for the rolling piston and scroll compressors (Figures 5 to 8) clarify the reasons for the trends observed for the thermodynamic efficiencies shown in Figure 4. The rolling piston compressor presents a monotonic behavior for the total thermodynamic loss as the condensing temperature increases. On the other hand, the scroll compressor presents an inverted U-shaped curve for the thermodynamic efficiency mainly due to under and over compression losses. Figures 5 to 8 also show that, regarding heat transfer, the main loss for the rolling piston compressor is related to the heating of the gas that occurs during the formation of the suction chamber, whereas for the scroll compressor the main loss related to heat transfer is associated with suction superheating. This is a result of the differences between the layouts of the rolling piston and scroll compressor shells.

Figures 9 and 10 present the mass flow rate and volumetric efficiency for the rolling piston and scroll compressors at different operating conditions. It can be noticed that the mass flow rate of both compressors is reduced as the condensing temperature increases, regardless of the evaporating temperature. This reduction of mass flow rate is more significant for the scroll compressor, especially for higher condensing temperatures. For this reason, the scroll compressor presents a higher volumetric efficiency than the rolling piston at lower condensing temperatures, but it eventually becomes lower as the condensing temperature is increased.

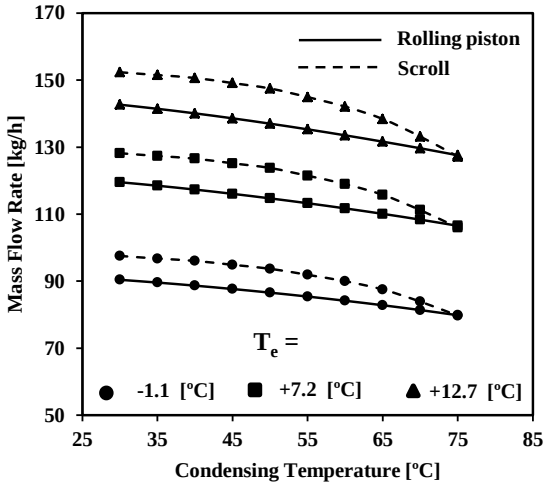

Figure 9: Mass flow rate for scroll and rolling piston compressors for different evaporating temperatures.

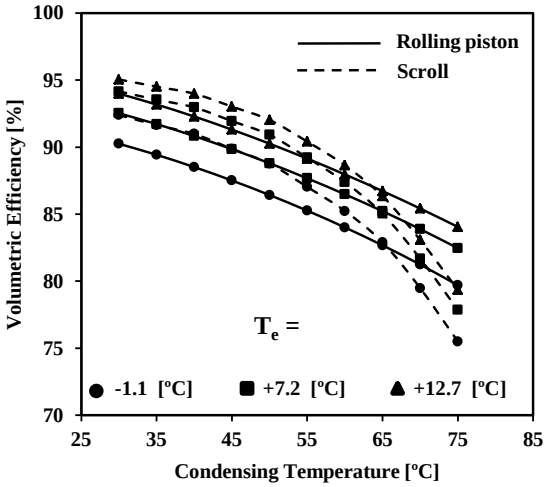

Figure 10: Volumetric efficiency of rolling piston and scroll compressor for different evaporating temperatures.

Opposite to what occurs for the energy losses, the mass losses inventories do not vary significantly with the evaporating temperature for the scroll and rolling piston compressors. For this reason, only the mass loss inventory for the evaporating temperature of T_e = +7.2 ºC is shown for both compressors in Figures 11 and 12. It can be observed that the mass losses present a linear increase for the rolling piston, while a non-linear pattern is observable for the scroll compressor, which is directly related to the increase of leakage and superheating at higher condensing temperatures. This explains the decrease of volumetric efficiency observed in Figure 10 for the scroll compressor..

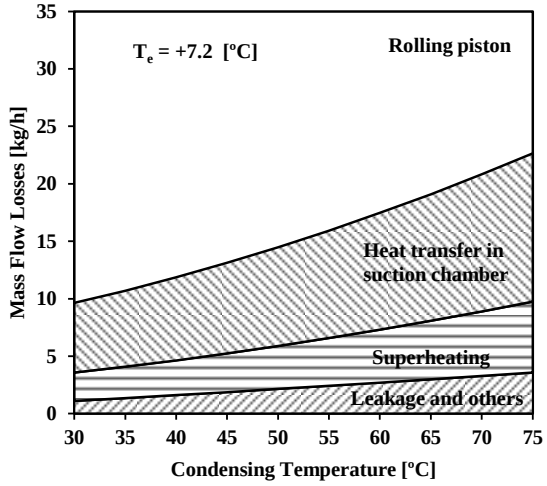

Figure 11: Mass losses for rolling piston at T_e = +7.2

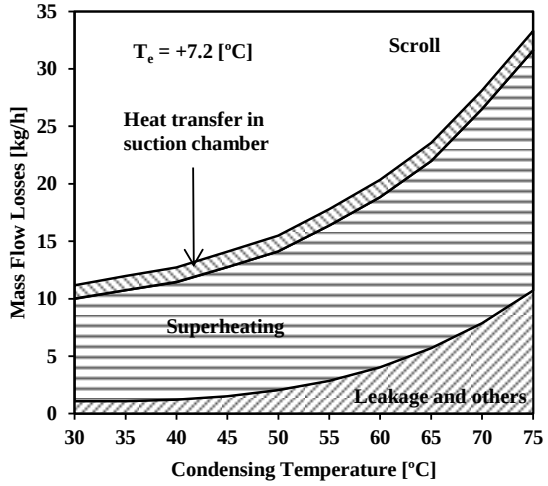

Figure 12: Mass losses for scroll at T_e = +7.2

6. CONCLUSIONS

This paper presented a comparative analysis of the thermodynamic efficiency of rolling piston and scroll compressors for air conditioning applications. To this extent, two compressors designed to operate at AHRI-A condition (T_e = 7.2 ºC and T_c = 54.4 ºC) were compared in different operating conditions that included MBP and HBP applications. Both compressors were initially experimentally analyzed and calculations of volumetric and global efficiency showed that the most efficiency compressor depends on the operating condition. Two validated simulation models were then adjusted and used to evaluate the thermodynamic and mass losses of each compressor. The analysis showed that the scroll compressor presents a better performance than the rolling piston compressor close to the design pressure ratio, which is related to the scroll geometry. Away from these operating points the scroll compressor shows a considerable decrease of efficiency, mainly due to under and over compression effects. It was also possible to identify that at higher evaporating temperatures the rolling piston compressors presents significant losses in the discharge process due to the higher mass flow rate. Finally, heat transfer was seen to significantly decrease the efficiency of both compressors.

NOMENCLATURE

General symbols

A	Area	[m^2]	T	Temperature	[ºC]
H	Heat transfer coefficient	[W/m^2K]	T_e	Evaporating temperature	[ºC]
$\dot{m}$	Mass	[kg]	T_c	Condensing temperature	[ºC]
$\dot{m}$	Mass flow rate	[kg/s]	$\forall$	Volume	[m^3]
h	Enthalpy	[J/kgK]	η_g	Electromechanical efficiency	[-]
p	Pressure	[Pa]	η_g	Global efficiency	[-]
$\dot{Q}$	Heat transfer rate	[W]	η_v	Volumetric efficiency	[-]

REFERENCES

Bezerra Jr, J. G., Deschamps, C. J., Silva, E. & Brancher, R. D. (2013). Thermodynamic performance of reciprocating and rolling piston compressors for heat pump application. *In: Proc. Int. Congress on Compressors*. Papiernicka, Slovak Republic.

Brancher, R. D. (2013). Development and validation of a model to predict the performance of rolling piston compressors (in Portuguese). *M.Sc. Thesis*, Federal University of Santa Catarina, Brazil.

Chua, K. J., Chou, S. K., Yang, W. M. & Yan, J. (2013). Achieving better energy-efficient air conditioning – A review of technologies and strategies. *Appl. Energy.*, 104, 87-104.

Diniz, M. C. & Deschamps, C. J. (2014). A NTU-based model to estimate suction superheating in scroll Compressors. *In: Proc. Int. Compressor Engineering Conference at Purdue University*, (paper 2325). West Lafayette, USA.

Dutra, T. & Deschamps, C. J. (2013). Experimental characterization of heat transfer in the components of a small hermetic reciprocating compressor. *Appl. Therm. Eng..*, 58, 499-510.

Gomes, A. R. & Deschamps, C. J. (2007). A thermodynamic analysis of scroll, rolling piston and reciprocating compressors for commercial refrigeration. *In: Proc. Int. Congress of Refrigeration*. Beijing, China.

Jang, K. & Jeong, S. (2006). Experimental investigation on convective heat transfer mechanism in a scroll compressor. *Int. J. Refrig.*, 29, 744-753.

Liu, Z. & Soedel, W. (1992). Modeling temperatures in high speed compressors for the purpose of gas pulsation and valve loss modeling. *In: Proc. Int. Compressor Engineering Conference at Purdue University*, (paper 932). West Lafayette, USA.

Maertens, M. J. & Richardson, H. (1992). Scroll compressor operating envelope considerations. *In: Proc. Int. Compressor Engineering Conference at Purdue University*, (paper 850). West Lafayette, USA.

Ooi, K. T. (2012). Compressor performance comparison when using R134 and R1234yf as working fluids. *In: Proc. Int. Compressor Engineering Conference at Purdue University*, (paper 2040). West Lafayette, USA.

Ooi, K. T. (2014). Twenty Years of Compressor Innovation at NTU, Singapore. *In: Proc. Int. Compressor Engineering Conference at Purdue University*, (paper 2384). West Lafayette, USA.

Orosz, J., Bradshaw, C. R., Kemp, G. & Groll, E. A. (2042). An update on the performance and operating characteristcs of a novel rotating spool compressor. *In: Proc. Int. Compressor Engineering Conference at Purdue University*, (paper 2327). West Lafayette, USA.

Padhy, S. K. & Dwivedi, S. N. (1994). Heat transfer analysis of a rolling-piston rotary compressor. *Int. J. Refrig.*, 17, 400-410

Pereira, E. L. L. (2012). Modeling and analysis of the thermodynamic performance of scroll compressors (in Portuguese). *Ph.D. Thesis*, Federal University of Santa Catarina, Brazil.

Pereira, E. L. L. & Deschamps, C. J. (2010). A lumped thermodynamic model for scroll compressors with special attention to the geometric characterization during the discharge process. *In: Proc. Int. Compressor Engineering Conference at Purdue University*, (paper 2007). West Lafayette, USA.

Pereira, E. L. L. & Deschamps, C. J. (2012). A numerical study of convective heat transfer in the compression chambers of scroll compressors. *In: Proc. Int. Compressor Engineering Conference at Purdue University*, (paper 2191). West Lafayette, USA.

Pereira, E. L. L. & Deschamps, C. J. (2015). Prediction of gas leakage through clearances in scroll compressors. *In: Proc. Int. Congress of Refrigeration*, (paper 2191). Yokohama, Japan.

ACKNOWLEDGEMENT

The present study was developed as part of a technical-scientific cooperation program between the Federal University of Santa Catarina and EMBRACO. The authors also acknowledge the financial support of EMBRAPII Unit POLO/UFSC and CAPES (Coordination for the Improvement of High Level Personnel).